The Effects of Electron and Hole Injection on the Photoluminescence of CdSe/CdS/ZnS Nanocrystal Monolayers

Ann K. Gooding, Daniel E. Gómez, and Paul Mulvaney*

School of Chemistry & Bio21 Institute, University of Melbourne, 3010, Victoria, Australia

ABSTRACT The photoluminescence (PL) of 2D monolayers of CdSe/CdS/ZnS semiconductor nanocrystals (NCs) deposited on gold substrates and incorporated into electrochemical cells has been studied. By combining simultaneous cyclic voltammetry and confocal microscopy it is demonstrated that when a positive potential is applied to the film in an acetonitrile electrolyte, the PL is irreversibly quenched. This is irrespective of whether the samples are under an inert atmosphere or exposed to air or water vapor. When a negative potential is applied under nitrogen, quenching is also observed; however, it is reversible. Conversely when a negative potential is applied to the NC films in aerated acetonitrile, the PL intensity increases. The enhancement of the PL is stable for at least 180 s while the potential is held at −1.0 V (*vs* Ag quasi-reference electrode). When the potential is removed the PL intensity returns to the starting value. These results clearly indicate that photobrightening and charge carrier injection are coupled processes. On the basis of these data, we propose a simple kinetic model that explains the origins of photobrightening.

KEYWORDS: semiconductor nanocrystals · photoluminescence · cyclic voltammetry · monolayers · charge injection · photobrightening · blinking · confocal microscopy.

Despite extensive efforts to improve our understanding of the photochemistry of small semiconductor nanocrystals (NCs), some basic phenomena such as the blinking of single semiconductor NCs and the photobrightening of NC ensembles under illumination continue to elude explanation. Initial studies of blinking have led to the proposal that semiconductor NCs are dark or nonemitting as a result of charging, which is caused by emission of a charge carrier into the surrounding matrix.[1,2] Other researchers suggest that it may be due to prolonged periods of charge carrier trapping in surface states.[3] Spectral diffusion is also observed in single NC studies. It has been postulated that this process maybe related to random electric fields created by fluctuations in the charge density near the nanocrystal surface.[4–6] A related phenomenon is photobrightening, which has likewise been explained in terms of surface states,[7] Auger processes,[8] ligand oxidation[9] and surface reconstruction.[10] To test these hypotheses concerning NC luminescence, it is necessary to study the emission from charged NCs. However injecting charge carriers using chemical techniques is not straightforward and has made verification of these models difficult. Consequently, the few published reports are somewhat contradictory and ambiguous.[11,12] For example, Guyot-Sionnest and co-workers see no change to the emission peak when the NCs are negatively charged with a single electron,[13] while other reports suggest that the injection of electrons and/or holes leads to quenching of the PL and results in surface-mediated anodic or cathodic dissolution of the crystal lattice.[14,15]

One approach, which has been very fruitful, is to employ dense, multilayer NC films as electrodes. Such films have optical densities large enough to enable absorption spectroscopy to be utilized. Applying this method to PbSe NCs, Guyot-Sionnest and co-workers have shown that electron injection leads to a bleaching of the ground-state exciton level owing to state-filling and the appearance of NIR intraband transitions.[16] However, in their report the PL of the samples was not measured so it is not possible to confirm whether this filling of the $1S_e$ state leads to significant changes in the NC luminescence. Brus *et al.* imaged CdSe NCs using electrostatic AFM while illuminating the NCs. Their data suggest a change in the charge of the NCs following bandgap illumination. However, the AFM technique does not distinguish between surface trapping of charge carriers and ionization of the nanocrystals.[17]

In this work, we follow changes in the PL spectra as a function of applied potential under atmospheres of both nitrogen and air. Charge injection is accomplished

*Address correspondence to mulvaney@unimelb.edu.au.

Received for review November 3, 2007 and accepted February 13, 2008.

Published online March 12, 2008.
10.1021/nn7003469 CCC: $40.75

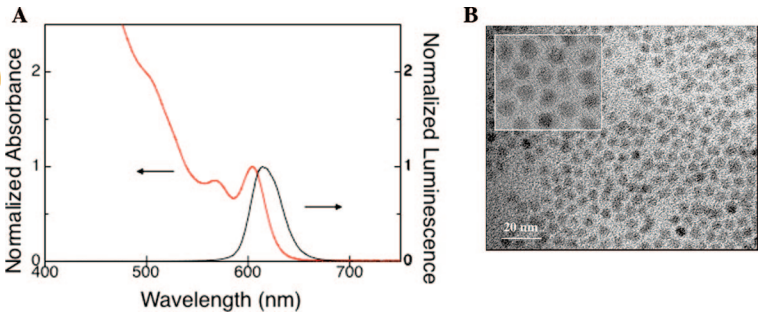

Figure 1. (A) Normalized absorbance (red line) and PL (black line) spectra of colloidal CdSe/CdS/ZnS nanocrystals in chloroform; (B) TEM image of 6.1 nm CdSe/CdS/ZnS nanocrystals.

with cyclic voltammetry and step-pulse voltammetry. Cyclic voltammetry has been used previously to probe the potential of the energy levels in NCs and to predict the band-gap energy.[18–20] Here, we use this technique to uniformly charge the NCs, which are organized as a 2D self-assembled monolayer on the working electrode. This arrangement minimizes the effects of electrostatic charging and carrier diffusion, which can occur in multilayer films and also allows us to control the amount of charge that is injected into each NC. Furthermore, the monolayer formation allows more rapid and reversible charge carrier injection. The disadvantage is that it is not possible to measure absorption changes with any accuracy. In this paper we demonstrate that excess charge carriers have a profound effect on the PL from CdSe/CdS/ZnS NCs. It is also shown that the environment plays a key role in the intensity of PL emitted from core–shell NCs. The results allow us to postulate a simple model for photobrightening of semiconductor nanocrystals.

RESULTS

The NCs studied in this report are in the form of self-assembled monolayers with an area of approximately 1.5 cm^2. The absorbance and PL spectra of the CdSe/CdS/ZnS core/shell NCs dispersed in solution are shown in Figure 1 A. Topographic atomic force microscopy images of the nanocrystals in self-assembled films show monolayer coverage over areas of tens of square micrometers.[21] The homogeneity of the PL emission and the uniform height are more apparent from images of patterned arrays of the CdSe/CdS/ZnS NCs. A typical example is shown in Figure 2. The NC monolayer thickness can be determined at different points of the patterned array using atomic force microscopy and these topographic measurements confirm that the nanocrystals adsorb as a densely packed monolayer and the emission intensity is extremely uniform over the surface of the film.

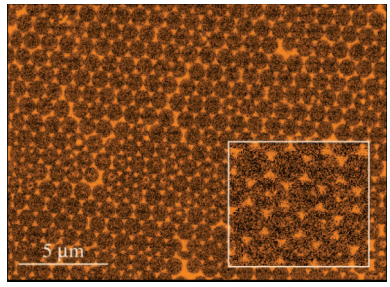

Figure 2. Confocal microscopy image of a monolayer of CdSe/CdS/ZnS nanocrystals.The nanocrystals are formed on a glass substrate with triangular gold "islands" *via* nanosphere lithography. The chemical linker (ethylenedithiol) only binds to the patterned gold areas.

Anodic Bias in Air or under N_2. The results of applying a positive potential to the electrochemical cell when it is open to air are shown in Figure 3. The initial stability of the PL is established in the time frame between 0 and ~200 s. At ~200 s, the potentiostat begins to scan from 0 to +1.8 V at a rate of 20 mV/s. The PL is immediately affected by the injection of positive charge and is completely quenched by the time the potential reaches 1.06 V. When the potential is returned to zero the monolayer remains dark (*i.e.*, nonfluorescent) indicating that the PL quenching is irreversible. Likewise under nitrogen, the same effects are observed, that is, a rapid quenching of the PL and no recovery upon reversal of the potential.

Cathodic Bias in N_2. Next, a monolayer of the core/shell NCs was negatively charged in an inert atmosphere with a degassed electrolyte. Figure 4A shows that the PL is partially quenched (by 65%) when the film is negatively charged in this system, reaching a minimum intensity at −1.25 V. The PL then returns to its original value when the potential is returned to 0 V. Analysis of the corresponding cyclic voltammogram reveals a small reduction peak (~0.1 mA) at −1.2 V (Figure 5). At negative potentials, the NC monolayer PL peak is observed to red-shift 2 nm (Figure 4B). It blue-shifts by 2nm when the potential is returned to 0 V.

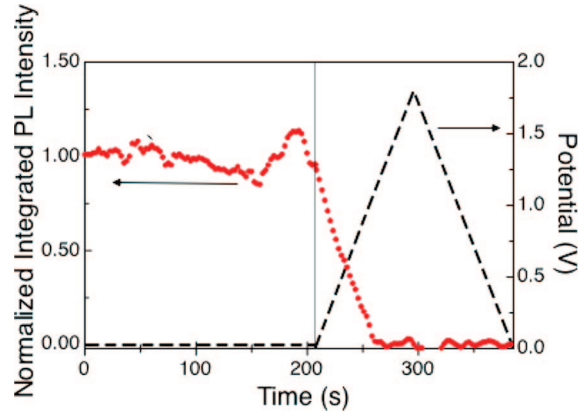

Figure 3. Integrated photoluminescence intensity (red circles) of a monolayer of CdSe/CdS/ZnS before and during positive charging in dry air. The black dashed line shows the potential applied to the working electrode as a function of time. The vertical line in the centre of the diagram highlights the moment the potential is switched on. The working electrode is immersed in 0.1 M $TBAPF_6$/acetonitrile solution. The potential is applied at a scan rate of 20 mV/s.

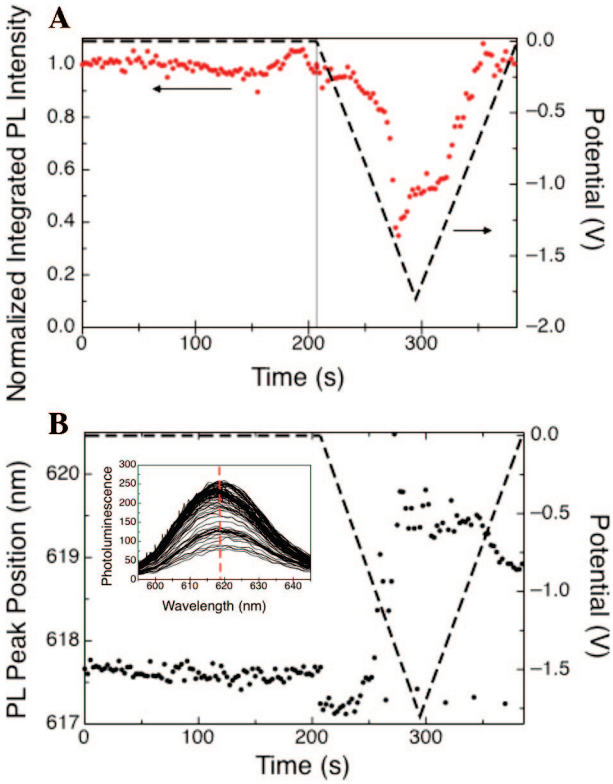

Figure 4. (A) Integrated photoluminescence intensity (red circles) from a monolayer of CdSe/CdS/ZnS nanocrystals as the film is negatively charged under dry nitrogen. The potential applied to the working electrode at any given time is shown as a black dashed line. (B) The position (wavelength) of the photoluminescence peak (black circles) during charging. Inset shows the PL spectra as a function of time. Potential scan rate is 20 mV/s; electrolyte is 0.1 M $TBAPF_6$/acetonitrile.

Cathodic Bias in Air. A very different effect is observed when the NC monolayer is subjected to a negative potential in aerated, acetonitrile electrolyte. As seen in Figure 6A, when the potential is initially scanned to negative values, the PL does not appear to change. However, once the potential reaches *ca.* −1.2 V, the PL undergoes a substantial enhancement (up to 200%) and remains at this higher intensity while the potential is increased to −1.8 V. Upon reversal of the potential, the PL progressively decreases until all the charge is removed. After one full cycle of the potential, the PL returns to a steady state, which is slightly lower than its starting value. Prior to charging, the PL maximum is located at 618 nm and when the cathodic potential is applied we observe a 2 nm red-shift in the PL maximum (Figure 6B). The inset in Figure 6B shows that there is no change to the shape of the emission peak during charging. This small peak shift is reversed when the potential is returned to zero.

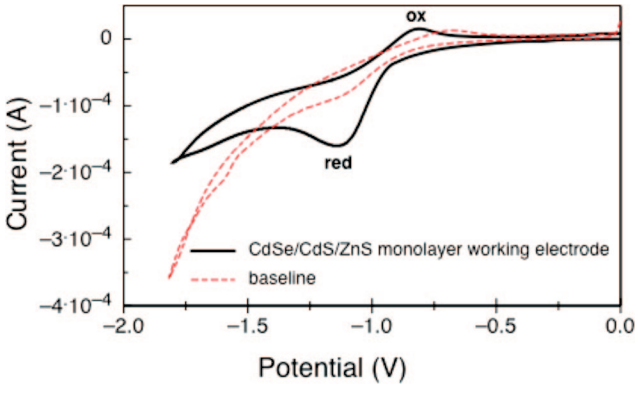

Figure 5. Cyclic voltammogram for a monolayer of CdSe/CdS/ZnS nanocrystals bound to a gold working electrode (1.5 cm_2). Reduction peak is seen at - 1.2 V. The counter electrode is a Pt wire and a Ag wire is used as the quasi-reference. Electrolyte is 0.1 M $TBAPF_6$ in acetonitrile (degassed with N_2). Scan rate 20 mV/s/.

Differential Pulse Voltammetry in Air. We used differential or step-pulse voltammetry to determine if the enhanced PL was stable over time. In Figure 7 it can be seen that the PL is not affected by the application of the −0.5 V potential step. However, when the potential is stepped to −1.0 V, the integrated PL suffers a sharp decrease but quickly recovers and then ultimately increases by 75% from its original value. The PL in this case begins to increase at a potential that is more positive than when cyclic voltammetry was used. The enhanced PL is shown to be stable at −1.0 V over a 180 s period. When the potential is returned to 0 V, the PL from the NC film is constant and the peak intensity returns to the original level.

DISCUSSION

The results from the above experiments demonstrate that CdSe/CdS/ZnS NCs respond very differently to positive and negative electrode potentials. However, the experiments also reveal that the response to charging is strongly linked to the environmental effects of gases and/or water vapor. It also appears as though the CdS/ZnS shell, which is 1.05 nm thick, does not affect the injection of charges to the CdSe core since electron injection occurs at potentials well below the predicted conduction band energy for bulk ZnS.

Hole Injection. When a positive potential is applied to the CdSe/CdS/ZnS monolayer the PL is irreversibly quenched. The irreversibility suggests that injected holes induce chemical decomposition of the CdSe, which is anodically unstable:[14]

$$CdSe + 2h^{+}_{vb} \rightarrow Cd^{2+} + Se \qquad (1)$$

Unfortunately we were not able to observe a blue shift of the PL peak position, which would confirm dissolution of the NCs. If the quenching is due to reaction 1, it is somewhat surprising since high resolution TEM shows that the CdSe cores are homogeneously coated with ZnS, which should inhibit oxidative dissolution. It is possible that corrosion occurs only at the

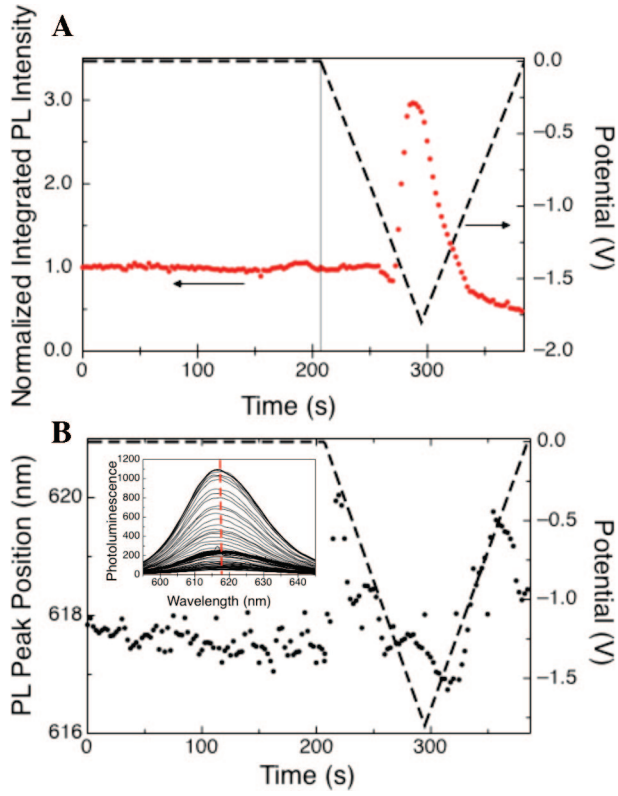

Figure 6. (A) Integrated photoluminescence intensity (red circles) of CdSe/CdS/ZnS nanocrystals under a negative potential in air. The black dashed line shows the applied potential. (B) The wavelength of the emission peak (black circles) as a function of the electrode potential. The inset shows the PL spectrum as a function of the potential. The electrolyte is 0.1 M $TBAPF_6$/acetonitrile and the scan rate is 20 mV/s.

internal CdSe/ZnS interface and that the lattice trapped Cd ions and Se atoms then act as dark recombination centers. Whether the holes are considered to charge the nanocrystals or simply to chemically oxidize them is a moot point. Regardless of the fate of the injected holes, one can infer that if free holes are present on the CdSe nanocrystals the PL will be drastically quenched (even if passivated by a semiconductor shell layer). This raises

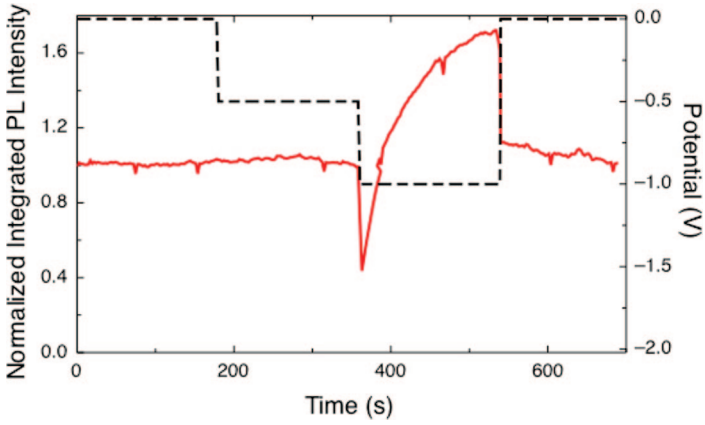

Figure 7. Differential pulse voltammetry of a CdSe/CdS/ZnS NC monolayer on a gold working electrode. Measurement was carried out in the presence of wet air. The red line is the integrated photoluminescence intensity of the film. The black dashed line shows the duration (time) of each potential step.

an interesting conclusion concerning the phenomenon of blinking. It has been frequently postulated that blinking is due to photoelectron emission into the environment around the nanocrystal. The NC is then assumed to be dark until the electron diffuses back to the NC. Our observation here is unambiguous. Injection of holes into CdSe/ZnS nanocrystals causes complete, irreversible PL quenching, whereas blinking involves rapid fluctuations in PL intensity. Hence it does not seem plausible that this mechanism accounts for blinking of single nanocrystals.

Electron Injection Under Nitrogen. The PL enhancement due to the injection of electrons is more difficult to explain since it is necessarily coupled to the nature of the environment. In previous studies where the NCs were negatively charged, the PL was quenched.[22,23] We also find that quenching occurs, but only under dry nitrogen. The cyclic voltammogram shows a reduction peak at −1.2 V, which is ascribed to the injection of electrons into the CdSe/CdS/ZnS NCs. This electrode potential is insufficient for injection into the ZnS shell, so the injected electrons may be considered to tunnel into the core. However, the electron wave function is delocalized across the core and shell. The PL peak at 605 nm corresponds to a 4.81 nm CdSe nanocrystal, while TEM shows the core to have a diameter of 4.0 nm.[24] Note that prior to charging, the PL is stable and we do not observe quenching until electrons are injected. The electrons reside either in the core LUMO ($1S_e$ state) or on surface traps. The fact that a very negative bias is applied before an injection current is observed suggests that the cross-section for direct injection into trap sites is extremely low. Guyot-Sionnest has previously observed bleaching of the $1S_e$ exciton level at –1.4 V for similar-sized nanocrystals using cyclic voltammetry.[25] He also reported the onset of new NIR transitions that correlate with excitation of $1S_e$ electrons to the $1P_e$ level, consistent with filling of the $1S_e$ level.[26]

There are therefore two possibilities for explaining the dark state of the *negatively* charged nanocrystals. If the injected electrons reside in the $1S_e$ state, then Auger recombination via the injected free carrier could lead to a loss of PL. Removal of the excess electrons during the CV scan would immediately lead to a recovery of the PL as observed. However, it is difficult to understand why water vapor can influence the NC PL by this mechanism. Instead, we argue that the first electrons are injected into the LUMO ($1S_e$) level, but immediately relax to surface acceptor sites (Scheme 1a, steps 1 and 2). Since ZnS passivation is extremely efficient, and since the PL is affected by water vapor, this trap state must be at the ZnS shell surface. Furthermore, this trapped state must correspond to a dark state of the entire NC. To explain why this is a dark state, we propose that the trapped electron has a large cross-section for the capture of photogenerated holes (Scheme 1b, step 3). These recombine nonradiatively at room tempera-

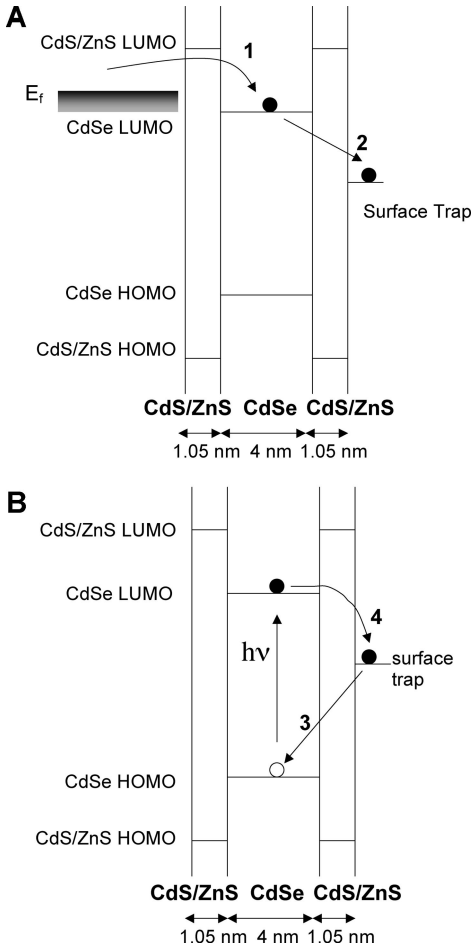

Scheme 1. Mechanism for the quenching of the photoluminescence from negatively charged NCs in nitrogen. (A) injection of an electron into the LUMO ($1S_e$) state of the NC core (1) and rapid relaxation to the empty surface trap (2); (B) light absorption creates an exciton. The photogenerated hole recombines nonradiatively with the trapped electron (3) and the photoelectron is retrapped at the surface via step 4.

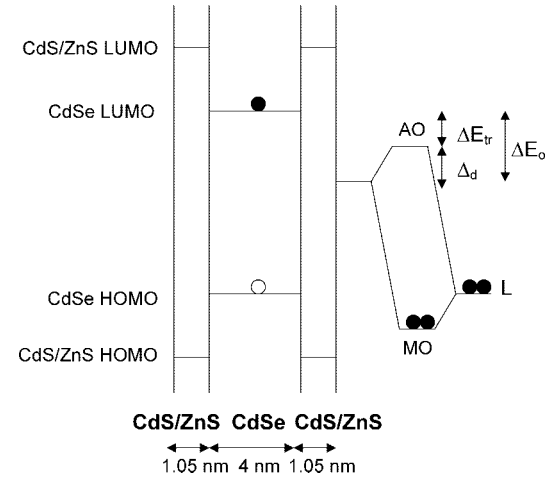

Scheme 2. The Interaction between a ligand, an exciton, and a surface electron trap. The intrinsic trap depth is E_o, but ligand adsorption raises the cadmium 5s antibonding orbital AO by Δ_d, making it less attractive for an electron to occupy this state. If the energy Δ_d exceeds E_o the surface trap energy is higher than the core LUMO and the trap is absolutely passivated.

ture and the residual LUMO electron then retraps at the same or another vacant surface site (step 4). This process leads to a perpetually dark NC, which will only become bright again once the excess electron is removed. The fact that a negatively charged NC can remain dark for long periods of time but recovers its PL upon extraction of the injected electrons provides a mechanism to explain blinking. A negatively charged nanocrystal can be photogenerated whenever a hole is removed by oxidation of a ligand or a lattice selenium ion. The trapped electron acts as a nonradiative recombination center. This behavior is consistent with the fact that CdSe is thermodynamically stable with respect to injection of electrons but is anodically unstable.

This raises the question, how many active surface traps are there? Guyot-Sionnest calculated that injection of only 1–2 electrons per particle led to bleaching of the ground-state exciton level.[25] This is possible only if the vast majority of vacant dangling bonds associated with the surface cadmium ion 5s orbitals are permanently occupied. The only mechanism that seems consistent with this is to postulate that virtually all solvent, gas, or surfactant molecules present in the environment, such as N_2, O_2, H_2O, and CO_2, can act as very weak Lewis bases and adsorb to any unpassivated CdSe surface sites, providing weak passivation of the nanocrystal surface.

In Scheme 2 we consider the interaction of an excited electron with a surface electron trap that is in equilibrium with a ligand. If the intrinsic trap depth is ΔE_o, the process of adsorption of the ligand through a dative bond, stabilizes the two lone pair electrons on the ligand by an amount of energy Δ_d, through the formation of a bonding molecular orbital, MO. The antibonding orbital (AO) is correspondingly raised in energy by Δ_d. The trap depth is reduced to $\Delta E_{tr} = \Delta E_o - \Delta_d$ and trapping is now unfavorable because occupation decreases the bond order. Hence, it is possible that photogenerated electrons will not occupy the AO while a ligand is adsorbed and the entire surface of the semiconductor NC is always passivated to some extent by environmental solvent or ligands. If the ligand adsorption is exothermic enough, the AO energy level may be raised above the LUMO level, and charge carrier trapping is not energetically feasible at all ($\Delta_d > \Delta E_o$). We will term this absolute passivation. For photostability, it is also important that the MO lies below the HOMO of the nanocrystal, otherwise it may act as a hole trap. This may be the case for thiol adsorption on CdSe.

For deeper trap states, the conduction electron may be able to drive desorption of a weakly adsorbed ligand. Photodesorption of small molecules such as CO_2, H_2O, and O_2 has often been observed for bulk II−VI semiconductors such as CdS and ZnO. If this process consists of a charge carrier in the LUMO expelling a

weakly bonded ligand, L, then the free energy for photodesorption, ΔE_{pd}, is roughly:

$$e-_{(LUMO)} + :L_{(ads)} \rightarrow e-_{(tr)} + :L_{(solv)}$$

$$\Delta E_{pd} = \Delta E_{tr} - 2\Delta_d \quad (2)$$

where the factor of 2 takes into account the loss of both lone pair electrons during desorption. The dark state reactions occurring in the CdSe/CdS/ZnS nanocrystal are:

$$CdSe/CdS/ZnS(e_{tr}^-) \xrightarrow{h\nu} e_{LUMO}^- + h_{HOMO}^+ + e_{tr}^- \quad (3)$$

$$h_{HOMO}^+ + e_{tr}^- \xrightarrow{h\nu} \text{heat} \quad (4)$$

$$e_{LUMO}^- + Cd_{(surf)}^{2+} \xrightarrow{k_1} e_{tr}^- \quad (5)$$

The dark state is reversible because CdSe/CdS/ZnS is stable against cathodic decomposition, at least for injection of 1–2 electrons. Filling of higher exciton states will eventually lead to formation of elemental cadmium, as observed for CdS.[27] Upon reversing the bias, the trapped electrons will slowly repopulate the LUMO level from the trap state and be transported to the gold electrode. From Figure 6, it is seen that most of the PL recovery follows the scanned potential, indicating a detrapping rate >1 Hz.

Electron Injection In Aerated Conditions. Negatively charging the NCs in aerated solutions leads to completely different observations. A strong PL enhancement is observed with a negative bias in these cases. It is crucial to highlight that immediately following the injection of electrons, quenching is observed. However, the onset of quenching is counteracted by a slower, but more intense photobrightening process that only occurs under aerated conditions. That this process is photobrightening, and not a simple chemical passivation, is confirmed by measurements performed at different laser intensities. The growth in PL is faster when the laser flux is higher. We believe that the injected electrons cause initial darkening because of surface trapping as discussed above, but following this, a second chemical process occurs, which is only possible in aerated conditions. Experiments with water-vapor-saturated nitrogen showed the same photobrightening effects, whereas dry oxygen did not lead to an enhancement in the PL. This extremely surprising observation is completely consistent with the results of Cordero *et al.*[28] who observed photobrightening of CdSe monolayers only in humid air and with the single NC blinking studies of Müller *et al.*, who found water vapor reduced blinking of single NCs in air.[29] It appears to contradict the results of Mews who found water and oxygen increased blinking.[30] On the basis of Scheme 2, we now postulate a mechanism for photobrightening.

The NC is in a dark state owing to the presence of a trapped electron, e_{tr}^-. Creation of a hole allows the trapped electron to be removed nonradiatively as observed above via reactions 3 and 4. However, in aerated solutions of acetonitrile, there are water molecules present and there is competition for the vacant trap site each time the trapped electron recombines with a hole. This is illustrated by

$$H_2O_{(solv)} + Cd_{(surf)}^{2+} \xrightarrow{k_2} Cd_{(surf)}^{2+} : H_2O_{(ads)} \quad (6)$$

Reaction 6 competes with reaction 5 in wet environments. Note that substantial brightening of the NCs does not occur immediately upon exposure to water vapor, but only after photolysis. We believe this indicates that water adsorbs weakly and only to vacant surface traps. The gradual passivation of these sites by ligands as trapped electrons are scavenged by holes reduces the rate of nonradiative recombination and leads to an increase in PL quantum yield. Conversely, it is often observed that the PL increases drastically simply upon exposure of the nanocrystals to strongly adsorbing ligands such as primary alkylamines. This can be explained if it is assumed that very strong ligands are able to drive trapped electrons back into the conduction band if the trap depth is shallow (the reverse of reaction 2). Hence addition of alkylamines and refluxing for long periods of time leads to *thermal* brightening of the NC. The PL continues to increase over hours.[31] This is due to the displacement of weaker passivants such as water by the alkylamines, which offer absolute passivation, and also to the slow, thermal expulsion of trapped electrons on shallow sites. In this case, the nanocrystal PL increases immediately without any need for illumination. However, once an electron is deeply trapped, the only way the NC can recover from the dark state is by removing the electron from the trapped state by reaction with a valence band hole. Thus the major role of light in photobrightening is to remove deeply trapped electrons that mediate nonradiative recombination. The rate of photobrightening is then controlled by the concentration of ligand present and the light intensity.

Typically we find that some several thousand excitons must be generated per NC before photobrightening reaches its peak. Each time a ligand chemisorbs to the NC, the electron is forced to find increasingly shallower trap sites and the NC "photoanneals". The light shuffles the surface ligands around by continually creating free electrons, which drives desorption of weakly adsorbed ligands. The holes then remove the trapped electrons and there is temporarily a vacant site for which ligands can compete. At the end of the photobrightening cycle, the surface is well passivated and the

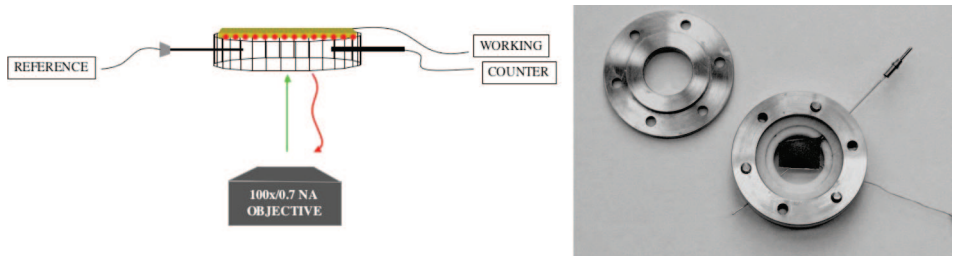

Figure 8. Schematic diagram of the voltametric cell used for simultaneous charging and microscopy of the nanocrystal monolayer on gold. The quasi-reference and counter electrodes contact the electrolyte solution through the walls of a Teflon ring. An Ar^+ laser irradiates the nanocrystals (on the working electrode) through the electrolyte.

injected electrons are probably more or less confined to the $1S_e$ exciton level, consistent with Guyot-Sionnest's observations for amine capped CdSe multilayer films under cathodic bias.

The Negatively Charged CdSe/CdS/ZnS Nanocrystals. After photobrightening under air/water vapor, the nanocrystals, which have been cathodically charged to −1.2 V are bright and exhibit higher PL yields than at the initial electrode potential. The observation that these negatively charged nanocrystals are bright implies that radiative recombination of negative excitons is more efficient than nonradiative Auger recombination. The 2 nm red-shift suggests that the Coulomb effects of the injected electron(s) on the PL emission energy are quite weak. Indeed, similar shifts have been predicted by Zunger *et al.*[32]

CONCLUSIONS

Positive and negative charge carriers have been injected electrochemically into CdSe/CdS/ZnS NC monolayers deposited onto working gold electrodes. It is found that positive charges (holes) lead to irreversible quenching of the NC PL, whereas the injection of an electron can induce two completely different effects. In an environment saturated with dry nitrogen, the PL is partially quenched but when the charged film is in contact with air the initially quenched PL undergoes photobrightening and the PL may be enhanced by a factor of 2 or more. Both of these processes are reversible, indicating that the NCs are chemically stable following the injection of small numbers of electrons. We conclude that even though the electrons are initially injected into the LUMO or $1S_e$ level, they are quickly trapped at the vacant surface sites, which leads to darkening of the NC. This process can be reversed by photolysis in the presence of ligands, which leads to photobrightening. Auger processes do not need to be invoked to explain the dark state. These results should enable further improvements in nanocrystal photostability, necessary for applications such as solar energy conversion and nanocrystal optoelectronics.[33]

MATERIALS AND METHODS

Chemicals. All chemicals were used as received without further purification. Cadmium oxide (CdO) (99.99%), selenium powder (99.99%), technical grade oleic acid (OA), octadecence (ODE), and trioctylphosphine (TOP) (90%) were purchased from Aldrich. Octadecylamine was obtained from (Merck, 90%), while bis (2,2,4,-trimethylpentyl) phosphinic acid (TMPPA) was procured from Cytec Specialty Chemicals. Elemental sulfur and zinc were used for the shelling steps. AR grade chloroform, acetone, and methanol were obtained from Univar. AR grade ethanol and acetonitrile were from Merck. We purchased 90% 1,2-ethanedithiol and tetrabutylammonium hexafluorophosphate ($TBAPF_6$) from Fluka.

Synthesis of Nanocrystals. The CdSe core particles were produced using established methods.[34,35] The resulting nanocrystals were transferred from the mother liquor into chloroform *via* extraction with acetone and methanol. To shell the 4.0 nm diameter CdSe NCs, the successive ion-layer adhesion and reaction (SILAR) procedure was used.[36–38] Briefly, the solution of washed, core NCs (9.52×10^{-5} M) was heated to 220 °C. At this temperature, 1.069 mL of Cd TMPPA (0.1 M) was injected, together with 0.6808 mL of OA, to make the NC surface cadmium rich. After 15 min, the temperature was raised to 225 °C, and a layer of sulfur was added (3.237 mL, 0.1 M). The solution was held at this temperature under nitrogen for 30 min. To form the graded seal shell structure, a CdZn layer was next deposited (1.619 mL of each metal, 0.1 M) and heated with a further 2.062 mL of OA for 15 min. This was followed by an addition of 5.897 mL of sulfur (0.1 M) and annealing at 235 °C for 30 min. At this same temperature, 5.897 mL of zinc/TMPPA (0.1 M) was added with 3.756 mL of OA. In total, four monolayers of shell material were deposited on the CdSe cores. This resulted in 6.1 nm diameter core/shell NCs that were annealed for 1 h at 200 °C, and then for 16 h at 80 °C. The first exciton peak absorbance of the final NC core/shells occurs at 605 nm, which is red-shifted by 20 nm from the preshelled cores ($\lambda_{max} = 585$ nm). This shift is consistent with the predicted values for an increase in the size of the NCs from 4.0 to 6.1 nm. Full details of the shelling process are given in a recent review.

Self-Assembled Monolayer Preparation. A film of gold (50 nm) was deposited on an acid-cleaned, glass substrate by sputter coating. The film was then immersed in ethylenedithiol (100 μM in ethanol) at room temperature for 1 h to form a self-assembled monolayer. The film was then rinsed well with ethanol and immersed in a concentrated solution of NCs (in chloroform) for 1 h. After thorough removal of the excess NCs with chloroform, the film was characterized via confocal microscopy.

Apparatus. Absorption measurements of the colloidal NCs were made on a Cary 5 UV–vis−NIR spectrophotometer. The emission spectrum was collected with a Cary Eclipse fluorescence spectrophotometer. A confocal microscope in epi-fluorescence mode was used to measure luminescence spectra from the self-assembled NC monolayer. The excitation source was the 488 nm line of an Ar^+ laser (7.7 μW), which was focused to a spot size of 355 nm with a 100×/0.7 NA objective (6 mm wd, Mitutoyo). The luminescence was collected and transferred to an imaging spectrograph equipped with a liquid-nitrogen-cooled CCD. With this setup, the temporal evolution of the luminescence peak position and integrated emission intensity were recorded at intervals of 1 s with a spectral resolution of ~0.09

nm. Two homemade electrochemical cells were employed for the electrochemistry measurements. One was open to the environment and the other was airtight and assembled under inert conditions. Both were specifically designed for use on the confocal microscope stage. Figure 8 shows the cell that is open to air. An Autolab PGSTAT 302 potentiostat was used for the cyclic voltammetry and differential pulse measurements. The working electrode in both systems was the as-prepared Au/self-assembled monolayer film. The counter and reference electrodes in all of the experiments were platinum and silver wires, respectively. All potential energies are quoted with respect to a silver wire quasi-reference electrode (we found ferrocene/ferrocinium, $E^{\circ} = 0.477$ V *vs* Ag q-ref).

Acknowledgment. A.K.G. thanks the Australian government for a postgraduate stipend. This work was carried out under ARC Grant DP0451651.

REFERENCES AND NOTES

1. Gómez, D. E.; Califano, M.; Mulvaney, P. Optical Properties of Single Semiconductor Nanocrystals. *Phys. Chem. Chem. Phys.* **2006**, *8*, 4989–5011.
2. Nirmal, M.; Dabbousi, B. O.; Bawendi, M. G.; Macklin, J. J.; Trautman, J. K.; Harris, T. D.; Brus, L. E. Fluorescence Intermittency in Single Cadmium Selenide Nanocrystals. *Nature* **1996**, *383*, 802–804.
3. Gómez, D. E.; van Embden, J.; Jasieniak, J.; Smith, T. A.; Mulvaney, P. Blinking and Surface Chemistry of Single CdSe Nanocrystals. *Small* **2006**, *2*, 204–208.
4. Blanton, S. A.; Dehestani, A.; Lin, P. C.; Guyot-Sionnest, P. Photoluminescence of Single Semiconductor Nanocrystallites by Two-Photon Excitation Microscopy. *Chem. Phys. Lett.* **1994**, *229*, 317–322.
5. Empedocles, S. A.; Norris, D. J.; Bawendi, M. G. Photoluminescence Spectroscopy of Single CdSe Nanocrystallite Quantum Dots. *Phys. Rev. Lett.* **1996**, *77*, 3873–3876.
6. Gómez, D. E.; van Embden, J.; Mulvaney, P. Spectral Diffusion of Single Semiconductor Nanocrystals: The Influence of the Dielectric Environment. *Appl. Phys. Lett.* **2006**, *88*, 154106-1–154106-3.
7. Sercel, P. C. Multiphonon-Assisted Tunneling Through Deep Levels: A Rapid Energy-Relaxation Mechanism in Nonideal Quantum-Dot Heterostructures. *Phys. Rev. B* **1995**, *51*, 14532–14541.
8. Efros, A. L.; Rosen, M. Random Telegraph Signal in the Photoluminescence Intensity of a Single Quantum Dot. *Phys. Rev. Lett.* **1997**, *78*, 1110–1113.
9. Kalyuzhny, G.; Murray, R. W. Ligand Effects on Optical Properties of CdSe Nanocrystals. *J. Phys. Chem. B.* **2005**, *109*, 7012–7021.
10. Wang, X.; Lianhua, Q.; Zhang, J.; Peng, X.; Xiao, M. Surface-Related Emission in Highly Luminescent CdSe Quantum Dots. *Nano Lett.* **2003**, *3*, 1103–1106.
11. Shim, M.; Wang, C.; Guyot-Sionnest, P. Charge-Tunable Optical Properties in Colloidal Semiconductor Nanocrystals. *J. Phys. Chem. B.* **2001**, *105*, 2369–2373.
12. Selmarten, D.; Marcus, J.; Rumbles, G.; Yu, P.; Nedeljkovic, J.; Shaheen, S. Quenching of Semiconductor Quantum Dot Photoluminescence by a π-Conjugated Polymer. *J. Phys. Chem. B* **2005**, *109*, 15927–15932.
13. Guyot-Sionnest, P.; Wang, C. Fast Voltammetric and Electrochromic Response of Semiconductor Nanocrystal Thin Films. *J. Phys. Chem. B* **2003**, *107*, 7355–7359.
14. Jasieniak, J.; Mulvaney, P. From Cd-Rich to Se-Rich—The Manipulation of CdSe Nanocrystal Surface Stoichiometry. *J. Am. Chem. Soc.* **2007**, *129*, 2841–2848.
15. Jones, M.; Nedeljkovic, J.; Ellingson, R. J.; Nozik, A. J.; Rumbles, G. Photoenhancement of Luminescence in Colloidal CdSe Quantum Dot Solutions. *J. Phys. Chem. B* **2003**, *107*, 11346–11352.
16. Wenrenberg, B. L.; Guyot-Sionnest, P. Electron and Hole Injection in PbSe Quantum Dot Films. *J. Am. Chem. Soc.* **2003**, *125*, 7806–7807.
17. Krauss, T. D.; Brus, L. E. Charge, Polarizability, and Photoionization of Single Semiconductor Nanocrystals. *Phys. Rev. Lett.* **1999**, *83*, 4840–4843.
18. Liu, D.; Kamat, P. V. Photoelectrochemical Behavior of Thin Cadmium Selenide and Coupled Titania/Cadmium Selenide Semiconductor Films. *J. Phys. Chem.* **1993**, *97*, 10769–10773.
19. Kucur, E.; Wendelin, B.; Giernoth, R.; Nann, T. Determination of Defect States in Semiconductor Nanocrystals by Cyclic Voltammetry. *J. Phys. Chem. B* **2005**, *109*, 20355–20360.
20. Haram, S. K.; Quinn, B. M.; Bard, A. Electrochemistry of CdS Nanoparticles: A Correlation between Optical and Electrochemical Band Gaps. J. *J. Am. Chem. Soc.* **2001**, *123*, 8860–8861.
21. Pacifico, J.; Gomez, D.; Mulvaney, P. A Simple Route to Tunable Two-Dimensional Arrays of Quantum Dots. *Adv. Mater.* **2005**, *17*, 415–418.
22. Wang, C.; Shim, M.; Guyot-Sionnest, P. Electrochromic Nanocrystal Quantum Dots. *Science* **2001**, *291*, 2390–2392.
23. Wang, C.; Shim, M.; Guyot-Sionnest, P. Electrochromic Semiconductor Nanocrystal Films. *Appl. Phys. Lett.* **2002**, *80*, 4–6.
24. Yu, W. W.; Qu, L.; Guo, W.; Peng, X. Experimental Determination of the Extinction Coefficient of CdTe, CdSe, and CdS Nanocrystals. *Chem. Mater.* **2003**, *15*, 2854–2860.
25. Wang, C.; Wehrenberg, B. L.; Woo, C. Y.; Guyot-Sionnest, P. Light Emission and Amplification in Charged CdSe Quantum Dots. *J. Phys. Chem. B* **2004**, *108*, 9027–9031.
26. Guyot-Sionnest, P.; Wehrenberg, B.; Dong, Y. Intraband Relaxation in CdSe Nanocrystals and the Strong Influence of the Surface Ligands. *J. Chem. Phys.* **2005**, *123*, 074709–1074709–7.
27. Spanhel, L.; Haase, M.; Weller, H.; Henglein, A. Photochemistry of Colloidal Semiconductors. 20. Surface Modification and Stability of Strong Luminescing CdS Particles. *J. Am. Chem. Soc.* **1987**, *109*, 5649–5655.
28. Cordero, S. R.; Carson, P. J.; Estabrook, R. A.; Strouse, G. F.; Buratto, S. K. Photo-Activated Luminescence of CdSe Quantum Dot Monolayers. *J. Phys. Chem. B* **2000**, *104*, 12137–12142.
29. Müller, J.; Lupton, J. M.; Rogach, A. L.; Feldmann, J.; Talapin, D. V.; Weller, H. Air-Induced Fluorescence Bursts from Single Semiconductor Nanocrystals. *Appl. Phys. Lett.* **2004**, *85*, 381–383.
30. Koberling, F.; Mews, A.; Basché, T. Oxygen-Induced Blinking of Single CdSe Nanocrystals. *Adv. Mater.* **2001**, *13*, 672–676.
31. Bullen, C.; Mulvaney, P. The Effects of Chemisorption on the Luminescence of CdSe QuantumDots. *Langmuir* **2006**, *22*, 3007–3013.
32. Franceschetti, A.; Zunger, A. Optical Transitions in Charged CdSe Quantum Dots. *Phys. Rev. B* **2000**, *62*, 16287–16290.
33. Gur, I.; Fromer, N. A.; Geier, M. L.; Alivisatos, A. P. Air-Stable All-Inorganic Nanocrystal Solar Cells Processed from Solution. *Science* **2005**, *310*, 462–465.
34. van Embden, J.; Mulvaney, P. Nucleation and Growth of CdSe Nanocrystals in a Binary Ligand System. *Langmuir* **2005**, *21*, 10226–10233.
35. Jasieniak, J.; Bullen, C.; van Embden, J.; Mulvaney, P. Phosphine-Free Synthesis of CdSe Nanocrystals. *J. Phys. Chem. B* **2005**, *109*, 20665–20668.
36. Li, J. J.; Wang, A.; Guo, W.; Keay, J. C.; Mishima, T.; Johnson, M. B.; Peng, X. Large-Scale Synthesis of Nearly Monodisperse CdSe/CdS Core/Shell Nanocrystals Using Air-Stable Reagents via Successive Ion Layer Adsorption and Reaction. *J. Am. Chem. Soc.* **2003**, *125*, 12567–12575.
37. Xie, R.; Kolb, U.; Li, J.; Basché, T.; Mews, A. Synthesis and Characterization of Highly Luminescent CdSe-Core CdS/Zn0.5Cd0.5S/ZnS Multishell Nanocrystals. *J. Am. Chem. Soc.* **2005**, *127*, 7480–7488.
38. van Embden, J.; Jasieniak, J.; Gomez, D. E.; Mulvaney, P. Review of the Synthetic Chemistry Involved in the Production of Core/Shell Semiconductor Nanocrystals. *Aust. J. Chem.* **2007**, *60*, 457–471.